THE JOURNAL OF BIOLOGICAL CHEMISTRY VOL. 287, NO. 1, pp. 712–722, January 2, 2012

Endosomal Accumulation of the Activated Epidermal Growth Factor Receptor (EGFR) Induces Apoptosis*

Received for publication, August 17, 2011, and in revised form, November 8, 2011 Published, JBC Papers in Press, November 18, 2011, DOI 10.1074/jbc.M111.294470

Jamie S. Rush[‡], Leslie M. Quinalty[‡], Luke Engelman[‡], David M. Sherry[‡§¶], and Brian P. Ceresa[‡1]

From the [‡]Department of Cell Biology, [§]Oklahoma Center for Neuroscience, and [¶]Department of Pharmaceutical Sciences, University of Oklahoma Health Sciences Center, Oklahoma City, Oklahoma 73106

Background: EGF receptor (EGFR) signaling is regulated by endocytosis.
Results: The intracellular localization of the EGFR affects its signaling.
Conclusion: EGFRs on the limiting membrane of endosomes, but not from the intraluminal vesicles, can induce apoptosis.
Significance: EGFR signaling is spatially regulated at multiple steps of the endocytic pathway.

Endocytosis positively and negatively regulates cell surface receptor signaling by temporally and spatially controlling interactions with downstream effectors. This process controls receptor-effector communication. However, the relationship between receptor endocytic trafficking and cell physiology is unclear. In MDA-MB-468 cells, cell surface EGF receptors (EGFRs) promote cell growth, whereas intracellular EGFRs induce apoptosis, making these cells an excellent model for studying the endocytic regulation of EGFR signaling. In addition, MDA-MB-468 cells have limited EGFR degradation following stimulation. Here, we report that in MDA-MB-468 cells the phosphorylated EGFR accumulates on the limiting membrane of the endosome with its carboxyl terminus oriented to the cytoplasm. To determine whether perturbation of EGFR trafficking is sufficient to cause apoptosis, we used pharmacological and biochemical strategies to disrupt EGFR endocytic trafficking in HeLa cells, which do not undergo EGF-dependent apoptosis. Manipulation of HeLa cells so that active EGF·EGFRs accumulate on the limiting membrane of endosomes reveals that receptor phosphorylation is sustained and leads to apoptosis. When EGF·EGFR complexes accumulated in the intraluminal vesicles of the late endosome, phosphorylation of the receptor was not sustained, nor did the cells undergo apoptosis. These data demonstrate that EGFR-mediated apoptosis is initiated by the activated EGFR from the limiting membrane of the endosome.

The EGF receptor (EGFR)[2] is the prototypical receptor tyrosine kinase and is found in virtually every tissue in the body. Binding of ligands, such as EGF, to the extracellular portion of the receptor triggers the activation of intracellular effectors (*i.e.* Shc, Grb2, PLCγ, PKC). The activities of these effectors integrate to modulate cell physiology. The liganded EGFR is known to alter cell proliferation, differentiation, migration, and survival. Functionally, these cellular changes influence developmental biology, wound healing, tissue homeostasis, and cancer biology (1, 2).

Signaling by the EGFR is a highly regulated process with a tight balance between the activation and inactivation of the receptor. Overexpression and hyperactivation of the EGFR are associated with a number of cancers, including those of the lung, colon, and kidney (3). Conversely, attenuation of EGFR kinase activity in patients using pharmacological inhibitors such as Iressa or Tarceva has been reported to disrupt epithelial homeostasis, resulting in colitis, dermatitis, and corneal erosions (4, 5). Thus, both too much or too little EGFR signaling can be deleterious.

The endocytic pathway is the primary molecular mechanism that maintains the balance in EGFR signaling. In addition to initiating the activation of downstream signaling pathways, EGF binding also causes the ligand-receptor complex to internalize via clathrin-coated pits. Once inside the cell, this cargo traverses the endocytic pathway by moving from clathrin-coated vesicles through early endosomes, late endosomes/multivesicular bodies, and lysosomes for degradation. This process is sufficient to attenuate EGFR signaling, but exactly how this occurs is unclear. Possible mechanisms include removing the receptor from the cell surface, dephosphorylating the receptor, sequestering the receptor away from downstream effectors, and targeting the ligand-receptor complex for degradation (6).

In addition, there are numerous reports in the literature that endocytosis is critical for the appropriate spatial localization of the ligand-receptor complex to activate downstream effectors (6). Inhibition of EGFR endocytosis decreases the efficiency of signaling to MAPK and PI3K (7) and induction of apoptosis (8). Further, maintaining the active EGFR at the plasma membrane enhances phosphorylation of EGFR, Shc, and PLCγ and DNA synthesis (7, 8). Although there are considerable biochemical data implicating a role for the endocytic pathway in the regulation of EGFR-effector communication, much less is known about the physiologic consequences of perturbing the spatial regulation of EGFR signaling. A more sophisticated under-

* This work was supported, in whole or in part, by National Institutes of Health Grants P20 RR 017703 from the COBRE Program of the National Center for Research Resources (to B. P. C.) and 1R01GM092874 (to B. P. C.). This work was also supported by Oklahoma Center for Advancement of Science and Technology Grant HR10-012 (to B. P. C.).

[1] To whom correspondence should be addressed: Department of Cell Biology, University of Oklahoma Health Sciences Center, Oklahoma City, OK 73106. Tel.: 405-271-8001, ext. 45508; Fax: 405-271-3548; E-mail: brian-ceresa@ouhsc.edu.

[2] The abbreviations used are: EGFR, EGF receptor; PARP, poly (ADP-ribose) polymerase; MTT, 3-(4,5-dimethylthiazol-2-yl)-2,5-diphenyl tetrazolium bromide; SiCon, control siRNA; LAMP2, lysosomal-associated membrane protein 2; ILVs, intraluminal vesicles.

standing of how the endocytic pathway regulates receptor signaling within the cell will provide critical insight into how to pharmacologically manipulate EGFR signaling.

We reported previously that in MDA-MB-468 cells, the EGF·EGFR complex must internalize for apoptosis to occur (8), indicating that intracellular signaling is required for EGFR-dependent induction of apoptosis. In contrast, when the EGF·EGFR complex is retained at the plasma membrane, there is enhanced DNA synthesis (8). These opposing effects on cell physiology by cell surface and intracellular EGFRs highlight the utility of MDA-MB-468 cells for studying the relationship between intracellular trafficking and signaling.

This study examines the molecular basis for apoptotic signals generated by intracellular EGFRs. Toward this end, we found that in MDA-MB-468 cells, the phosphorylated EGFR accumulates in the early endosome. These receptors are oriented on the limiting membrane of the early endosome so that phosphotyrosines of the carboxyl terminus are exposed to the cytoplasm. The accumulation of EGFRs on the limiting membrane of the endosomes is sufficient to produce EGFR-dependent apoptosis. Using HeLa cells that do not normally undergo apoptosis in response to EGF, we biochemically and pharmacologically recapitulated this defect in EGFR trafficking. The accumulation of EGFRs on the endosomal limiting membrane, but not in intraluminal vesicles, was sufficient to induce EGFR-mediated apoptosis. Thus, we have identified a way to alter EGFR-modulated cell physiology through manipulation of the endocytic trafficking of the receptor.

EXPERIMENTAL PROCEDURES

Cell Lines—MDA-MB-468 cells were obtained from the ATCC and maintained in DMEM, 10% FBS, 100 units/ml penicillin, 100 μg/ml streptomycin, and 2 mM glutamine. HeLa cells were a gift of Sandra Schmid (The Scripps Research Institute) and were maintained in DMEM containing 5% FBS, 100 units/ml penicillin, 100 μg/ml streptomycin, and 2 mM glutamine (9). Cell lines were maintained at 37 ° in 5% CO_2.

Percoll Gradient Fractionation—Analysis of radioligand distribution was performed as described by Kornilova *et al.* (10). Briefly, HeLa cells were incubated for 15 min with ^{125}I-EGF (1 ng/ml) at 37 °C in binding buffer (DMEM, 20 mM HEPES, 0.1% bovine serum albumin (pH 7.4)). Following treatment, cells were washed three times with PBS and returned to 37 °C in growth media. After another 45 min (60 min total), cells were washed twice with TES (10 mM triethanolamine, 1 mM EDTA, 0.25 M sucrose (pH 7.2)) and harvested in 2 ml of TES. Lysates were pipetted up and down 40 times and centrifuged for 10 min at 200 × *g* in a Sorvoll JA25.5 rotor. The supernatant was transferred to a clean tube and the pellet was resuspended in 2 ml of TES and centrifuged again. The resulting 4 ml of postnuclear supernatant was diluted with a 90% Percoll solution in TES to 17% in 11.5 ml. Samples were centrifuged for 25 min at 4 °C at 50,000 × *g* in a Beckman Ti65 rotor to separate early and late endocytic compartments. Samples were fractionated into 10-drop fractions (~30 fractions/gradient) from the bottom and measured for radioactivity in a Beckman γ counter. Data are plotted as the percentage of total radioactivity in each tube *versus* the relative migration of each fraction in the sample. Density was monitored using density marker beads (Amersham Biosciences).

In experiments using MDA-MB-468 cells, cells were treated with 10 ng/ml EGF for the indicated periods of time. Postnuclear supernatant was prepared as described above, resolved on a 17% Percoll gradient, and fractionated. Every other fraction was immunoblotted for phosphorylated EGFR, an early endosomal marker (transferrin receptor (TfnR)), and a late endosome/lysosome marker lysosome-associated membrane protein (LAMP-2)) as indicated in the figure.

Indirect Immunofluorescence—In experiments determining the endosomal orientation of the EGFR, cells were fixed in 4% paraformaldehyde and permeabilized with 0.015% digitonin, which permeabilizes the plasma membrane but not intracellular compartments (11). Cells were then incubated with EGFR antibodies that target either an amino-terminal epitope (AB-1, Calbiochem, San Diego, CA) or a carboxyl-terminal epitope (SC-03, Santa Cruz Biotechnology, Santa Cruz, CA). As a control to confirm the ability of both antibodies to label internalized EGFRs, cells were permeabilized with 0.1% saponin, which permeabilizes the limiting membrane to give access to the intraluminal compartment of the endosome. Confocal imaging was performed using an Olympus FluoView1000 confocal microscope with a ×60 oil immersion objective lens (numerical aperture 1.42, Olympus America, Center Valley, PA). For each condition, cells of interest were identified, and short stacks of images (1–3 μm total thickness in the *Z* dimension) were collected using a step size of 0.3 μm, yielding a *Z* resolution of ~0.3 μm for each optical plane within the stack. To ensure that images collected from all specimens were equivalent, hardware acquisition parameters were optimized for imaging cells under control conditions (no digitonin, no EGF treatment), and all acquisition parameters were then held constant for imaging cells under the remaining experimental treatment conditions. Channels were imaged sequentially to ensure that there was no bleedthrough of signals. No further adjustment of brightness, contrast, or threshold was performed. Images of individual optical planes from each experimental condition were exported to Adobe Photoshop for preparation of figures.

In experiments examining the accumulation of total EGFR distribution with and without monensin treatment (Fig. 7), the cells were permeabilized with 0.1% saponin after fixation but prior to processing with antibodies, as described previously (12). Images were collected on an Olympus IX70 microscope using a ×40 objective and a QiCam charge-coupled device camera controlled through Q-Capture software.

siRNA Oligo and Transfection—Both RAB7 and TSG101 siRNAs were described previously (23, 25). RAB7 siRNA was siGenome SMARTpool RAB7a preparation obtained from Dharmacon (Lafayette, CO). siRNA for TSG101 was obtained from Integrated DNA Technologies (Coralville, IA) using the published sequence. Transfection of HeLa cells was performed using Interferin® following the manufacturer's instructions.

Cell Lysate Preparation and Immunoblotting—Cell lysates were generated by washing the cells twice with PBS and solubilizing cells in lysis buffer (150 mM NaCl, 1% Nonidet P-40, 0.5% deoxycholate, 0.1% SDS, 50 mM Tris (pH 8.0), 10 mM sodium pyrophosphate, 100 mM sodium fluoride, 2 mM phenylmethyl

sulfonyl fluoride) on ice. Proteins were solubilized by rotating the lysis buffer/cell mixture end over end for 10 min at 4 °C. Insoluble material was removed by centrifugation for 10 min at 4 °C. The protein concentration of the solubilized protein was assessed by BCA assay (Pierce), and samples were diluted in SDS sample buffer. Equivalent amounts of protein (indicated in the figure legends) were separated by SDS-PAGE, transferred to nitrocellulose, and detected with the indicated antibody. Antibodies and sources are as follows: RAB7 (Sigma), TSG101 (Genetex, Irvine, CA), transferrin receptor (BD Transduction Laboratories), EGFR (SC-03, Santa Cruz Biotechnology), EGFR phosphotyrosine 1068 (Cell Signaling Technology, Danvers, MA), poly(ADP-ribose) polymerase (PARP) (Santa Cruz Biotechnology), lysosomal-associated membrane protein 2 (LAMP2) (University of Iowa Hybridoma Bank), and α-tubulin (Sigma). Antibodies were subsequently probed with horseradish peroxidase-conjugated goat anti-mouse or goat anti-rabbit secondary antibody (Pierce), and detected proteins were visualized by ECL using a UV Products imaging system. Band intensities were quantified using National Institutes of Health ImageJ software.

Radioligand Degradation—Cells were incubated for 7 min with 1 ng/ml ^{125}I-EGF (PerkinElmer Life Sciences, catalog no. NEX160; specific activity 150–200 μCi/μg) at 37 °C in binding buffer (DMEM, 20 mM HEPES, 0.1% bovine serum albumin (pH 7.4)). Cells were washed four times in room temperature PBS to remove unbound ^{125}I-EGF. Prewarmed 37 °C medium was added to the cells, and they were returned to 37 °C for the indicated periods of time. At each time point the medium was collected. The remaining cells were solubilized in 1% Nonidet P-40/20 mM Tris (pH 7.4). Cell lysates were incubated with 10% trichloroacetic acid and 1% BSA as a carrier protein on ice for 1 h. Intact protein was separated from degraded protein by centrifugation for 15 min at 14,000 rpm at 4 °C. The radioactivity for each of the three fractions (secreted, intact, degraded) was measured using a Beckman γ counter (13).

MTT Assays—For cells transfected with siRNA, HeLa cells were replated at a density of 5000 cells/well in a 96-well dish in 0.5% FBS, DMEM, 100 units/ml penicillin, 100 μg/ml streptomycin, and 2 mM glutamine 24 h after transfection. Six hours later, the medium was supplemented to achieve the indicated final concentration of EGF (0–10 ng/ml) or 5% FBS. After an additional 48 h, cell viability was measured using MTT (3,[4,5-dimethylthiazol-2-yl]-2,5-diphenyltetrazolium bromide) (14).

In cells treated with monensin, cells were plated at a density of 5000 cells/well in 0.5% FBS, DMEM, 100 units/ml penicillin, 100 units/ml streptomycin, and 2 mM glutamine. Six h later, the cells were pretreated with 5 μM monensin in DMEM and 0.05% methanol. Control cells were treated with 0.05% methanol in DMEM. Thirty minutes later, the medium was supplemented to achieve the indicated final concentration of EGF (0–10 ng/ml) or 5% FBS.

Data were plotted as the ratio of number of cells relative to cells in DMEM alone (0 ng/ml EGF). Statistics were calculated using Prism software (GraphPad Software, Inc., San Diego, CA).

RESULTS

Active EGFRs Accumulate in Early Endosomes in MDA-MB-468 cells—MDA-MB-468 cells are a unique model system for studying the spatial regulation of EGFR signaling. MDA-MB-468 cells were first described by Cailleau *et al.* (15) as part of a series of metastatic breast cancer cell lines derived at the M. D. Anderson Cancer Center in Houston, TX and are characterized by overexpression of EGFRs ($\sim 1.3 \times 10^6$ EGFRs/cell) (16). Like many cell lines expressing high levels of EGFRs, the endocytic trafficking of the receptor is delayed dramatically. The high level of receptor expression is favorable for studying the spatial regulation of EGFR signaling for two reasons. First, EGF treatment yields robust responses in terms of receptor phosphorylation, effector activation, and changes in cell biology. Second, the endocytic trafficking is naturally slowed because of saturation of the endocytic machinery. This allows one to differentiate between the duration of signaling and the spatial placement of the receptor.

In the case of MDA-MB-468 cells, a key cellular change accompanying treatment with EGF is the induction of apoptosis. Although EGF is typically thought of as a mitogenic growth factor, it is well established that EGF induces apoptosis in cells overexpressing the EGFR (17–19). However, the mechanism by which this occurs is not well understood.

Using MDA-MB-468 cells, we discovered that intracellular EGFRs, but not the cell surface receptors, induce apoptosis. Further, during the induction of apoptosis, there is little degradation of the EGF·EGFR complex. This led us to hypothesize that the intracellular accumulation of the active EGF·EGFR complex mediated the induction of apoptosis (8).

Because there is little degradation of the EGF·EGFR complex in MDA-MB-468 cells and the enhanced stability of the complex is associated with the induction of apoptosis, we wanted to know where in the endocytic pathway the complex accumulated. To answer this question, we treated MDA-MB-468 cells with EGF for varying amounts of time (15 min, 2 h, 16 h, or 24 h) and resolved the postnuclear supernatant on a 17% Percoll gradient to separate early and late endosomes. Following fractionation of the gradient, each fraction was probed by immunoblot analysis to determine the relative distribution of the phosphorylated EGFR at each time point (Fig. 1). At all time points, the phosphorylated EGFR accumulated overwhelmingly in fractions that corresponded to the early endosome, as indicated by the colocalization of the transferrin receptor (*TfnR*). In addition, the EGFR is segregated from lysosomal-associated membrane protein 2 (*LAMP2*), indicating that the majority of EGFR is segregated from the late endocytic pathway.

Previous studies demonstrated that there is very little ligand-stimulated EGFR degradation in MDA-MB-468 cells (8). Together with our gradient analysis, these data indicate that EGFR trafficking is blocked at the early endosome in MDA-MB-468 cells.

We next wanted to identify the orientation of the EGFR in the early endosomes. Under physiological conditions, when the EGFR is in the early endosome, it is located in the limiting membrane and oriented so that the ligand-binding amino terminus is in the lumen of the vesicle and the carboxyl-terminal

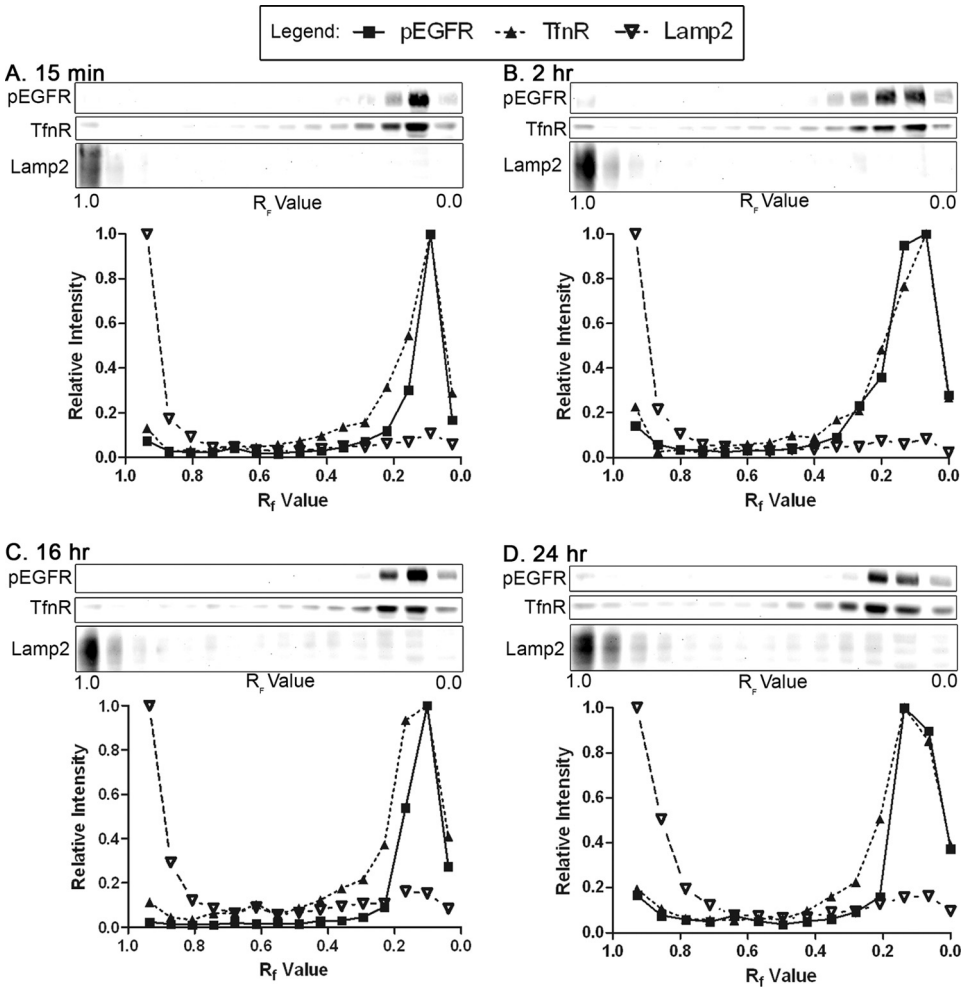

FIGURE 1. **EGF treatment of MDA-MB-468 cells causes the receptors to accumulate in the early endosome.** MDA-MB-468 cells were treated with 10 ng/ml EGF for 15 min (*A*), 2 h (*B*), 16 h (*C*), or 24 h (*D*). Postnuclear supernatants were prepared, run on isotonic 17% Percoll gradients, and fractionated into ~30 fractions (~330 ml each). Every other fraction was resolved by 7.5% SDS-PAGE, transferred to nitrocellulose, and probed with antibodies against the phosphorylated EGFR, the transferrin receptor (*TfnR*), and lysosomal-associate membrane protein 2 (*LAMP2*). Densitometric measurements of the immunoblot analyses were performed using National Institutes of Health ImageJ software, and the intensities were normalized to the maximum value and plotted for each fraction as indicated by the legend. Data shown are from representative experiments repeated for each time point in triplicate.

domain is oriented toward the cytoplasm. However, given the slowed kinetics of EGFR trafficking in MDA-MB-468 cells, we could not rule out the possibility that the EGF·EGFR complex in MDA-MB-468 cells had entered into intraluminal vesicles (ILVs), such as the multivesicular bodies that are characteristic of the late endosome, which would alter the orientation of the receptor termini. This difference in orientation is potentially very important, as it may alter receptor signaling.

Confocal microscopy of cells double immunolabeled using amino- and carboxyl terminus-specific EGFR antibodies was performed to determine whether the liganded EGFR was located on the limiting membrane or sequestered within the early endosome (Fig. 2). Cells were treated with EGF and fixed at intervals between 0 and 24 h to allow receptor internalization and trafficking to different portions of the endocytic pathway. After fixation, cells were treated with 0.015% digitonin to permeabilize the cell membrane while preserving the integrity of intracellular membranes. This procedure permits large molecules such as antibodies to penetrate the cell membrane but not the membranes of intracellular organelles (11). Under these conditions, only the terminus of internalized EGFR that is exposed to the cytoplasm will be available for antibody labeling, allowing assessment of the orientation of internalized receptors. To specifically identify the orientation of the amino and carboxyl termini of internalized EGFR receptors, the cells were incubated with an amino terminus-specific antibody (Ab-1, Calbiochem, mouse monoclonal, visualized with Alexa Fluor 568 (*red*)) in combination with a carboxyl terminus-specific antibody (SC-03, Santa Cruz Biotechnology, rabbit polyclonal, visualized with Alexa Fluor 488 (*green*)). At all time points, the amino terminus-specific EGFR antibody (*red*) strongly labeled the plasma membrane but showed little labeling within the cytoplasm (Fig. 2*A*). Following EGF treatment, the carboxyl terminus-specific EGFR antibody (*green*) stained EGFRs in the plasma membrane as expected, in addition to internalized receptors in endosomes (Fig. 2*B*).

The observed differences in EGFR labeling intensity may reflect the accessibility of the respective epitope (less intense staining) or concentration of receptors (more intense staining). Nevertheless, comparison of the relative distribution of each

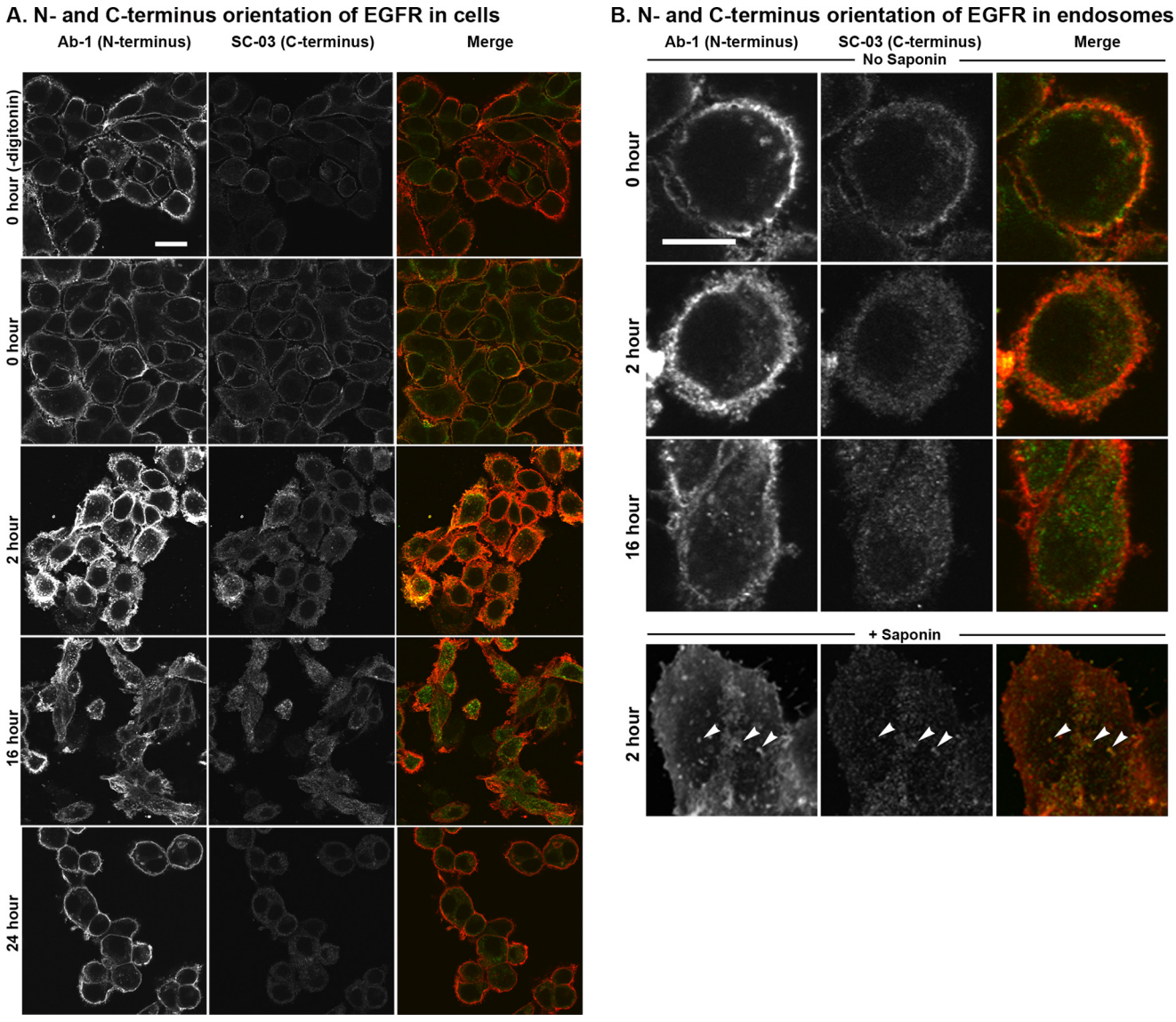

FIGURE 2. **EGF stimulated EGFRs in MDA-MB-468 cells accumulate on the limiting membrane of endosomes with the carboxyl terminus oriented toward the cytoplasm.** *A*, serum-starved MDA-MB-468 cells were treated with 10 ng/ml EGF for the indicated times, fixed, and treated with or without 0.015% digitonin to permeabilize the cell membrane while leaving the limiting membranes of intracellular organelles intact. Cells were fixed and processed for double indirect immunofluorescence with an EGFR amino terminal antibody (Ab-1, *red*) and an EGFR carboxyl-terminal antibody (SC-03, *green*) as described under "Experimental Procedures." Labeling for the amino terminus of the EGFR is present on the cell membrane at all time points but is absent from endosomal compartment in the cytoplasm. In contrast, labeling for the carboxyl terminus is present in both the cell membrane and in the endosome with longer EGR treatments, indicating that the C terminus of the internalized receptor is oriented toward the cytoplasm. Shown are representative single optical sections from an experiment performed three times. *Scale bar* = 20 μm. *B*, magnified images of data collected as described in *A*. Included is a positive control of cells permeabilized with 0.1% saponin to demonstrate endosomal staining with the amino-terminal specific EGFR antibody (Ab-1). *Scale bar* = 5 μm.

antibody reveals that the amino-terminal antibody primarily stains the plasma membrane and the carboxyl-terminal antibody stains the endosomes of 0.015% digitonin-permeabilized cells. Thus, the EGFR accumulates on the limiting membranes of the early endosome.

Pharmacological Disruption of EGFR Endocytic Trafficking Is Sufficient to Yield EGF-dependent Apoptosis—Having identified the defect in EGFR endocytic trafficking in MDA-MB-468 cells, we wanted to know whether disrupting endocytic trafficking at this stage was sufficient to make cells undergo EGF-dependent apoptosis. For these studies, we used human cervical cancer cells (HeLa cells) as a model system, as they do not normally undergo EGF-dependent apoptosis. HeLa cells express physiological levels of EGFRs (~50,000 EGFRs/cell) (20) and are amenable to genetic manipulation. The EGFR trafficking in HeLa cells has been characterized in detail (21–23), making these cells an excellent model for our studies.

A pharmacologic approach for our initial studies was a logical first step, as drugs can be added to cells via the medium and quickly perturb trafficking. We disrupted EGFR trafficking using the reversible ionophore monensin to block the acidification of the early endosome (24), which is essential for trafficking of the EGFR beyond the endosome.

Following treatment with monensin, the EGF·EGFR complexes accumulate in endosomes, as demonstrated by indirect immunofluorescent staining of the EGFR. This distribution is sustained for 180 min after EGF treatment (Fig. 3*A*). In contrast, vehicle-treated cells only transiently localize the

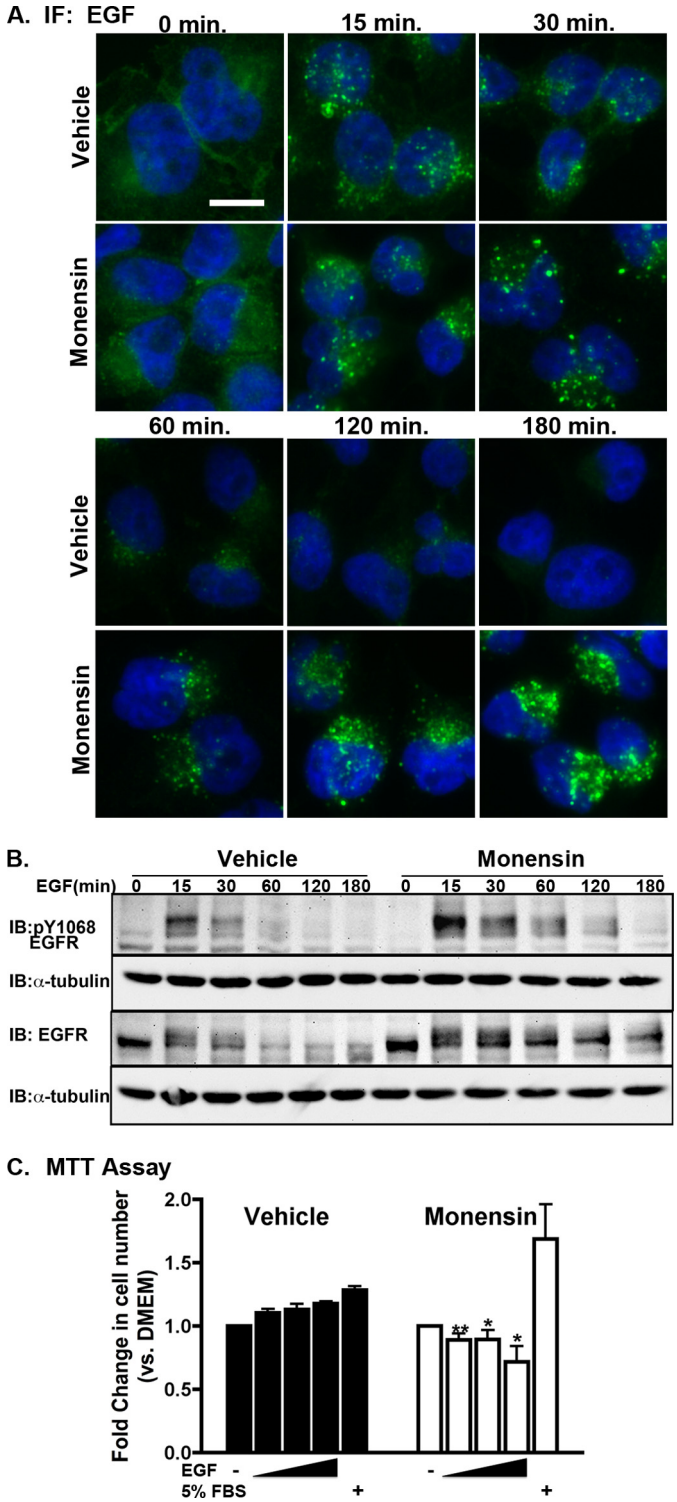

FIGURE 3. **Endosomal accumulation of the EGFR by monensin treatment is sufficient to promote EGF-dependent apoptosis.** *A*, HeLa cells grown on coverslips were pretreated with or without 5 μM monensin for 30 min, followed by treatment with 10 ng/ml EGF in the presence or absence of 5 μM monensin. At the indicated time points, the cells on the coverslip were fixed and processed for indirect immunofluorescence (*IF*) using an EGFR antibody (Ab-1) (*green*). Nuclei were stained with DAPI (*blue*). *Scale bar* = 10 μM. *B*, HeLa cells were pretreated with 5 μM monensin for 30 min, followed by treatment with 10 ng/ml EGF as indicated. Cell lysates were prepared, resolved by 7.5% SDS-PAGE, and immunoblotted (*IB*) with the indicated antibodies. *C*, HeLa cells were plated in 96-well dish, pretreated with 5 μM monensin for 30 min, and then stimulated with the indicated concentrations of EGF in DMEM or 5% serum in DMEM for 48 h in the absence or presence of 5 μM monensin. The number of viable cells was quantified by MTT assay. Data are plotted as the relative change in the number of cells as compared with cells maintained in DMEM. Data are presented as the average ± S.E. ($n = 4$). *, $p < 0.05$ calculated by a paired Student's *t* test.

EGF·EGFR complex to endosomes. With longer treatment times in vehicle treated cells, the staining for the EGFR becomes more diffuse. Monensin-treated cells have sustained EGF-stimulated EGFR phosphorylation and a slowed rate of ligand-stimulated EGFR degradation (Fig. 3*B*). This trafficking phenotype mimics what is observed in MDA-MB-468 cells.

To determine whether monensin treatment causes cell death in an EGF-dependent manner, we assessed cell viability in response to EGF by MTT assay (Fig. 3*C*). In monensin- but not vehicle-treated cells, EGF causes a dose-dependent decrease in the number of viable cells. The presence of monensin did not cause a statistically significant difference in the growth of cells with FBS. Thus, pharmacologically induced retention of the activated EGFR in the endosome is sufficient to cause cell death. However, it is not clear whether monensin-treated HeLa cells accumulate the EGFR on the limiting membrane of endosomes or sequestered in ILVs.

TSG101 and RAB7 Knockdown Disrupt EGFR Trafficking at Different Endocytic Stages—To determine whether the endosomal accumulation of the activated receptor was sufficient for EGFR-mediated apoptosis or whether the activated receptor had to be localized to the limiting membrane of the endosome, we used an RNAi strategy to knock down proteins that regulate distinct stages of endocytic trafficking. This experiment also served as a control for any nonspecific effects of monensin.

TSG101 is part of the endosomal sorting complex required for transport machinery. Specifically, it recognizes the liganded, ubiquitylated EGFR and directs it into the ILVs of the late endosome. Knockdown of TSG101 results in the accumulation of the EGFR on the limiting membrane of the late endosome (25). Under these conditions, the liganded EGFR is oriented with the carboxyl terminus of the receptor in the cytoplasm of the cell and presumably has access to downstream effector proteins, similar to what is observed in MDA-MB-468 cells.

The second protein, RAB7, is a small molecular weight G protein that is required for fusion of the late endosome and lysosome. Knockdown of RAB7 results in an enlarged late endosome containing an increased number of ILVs and the EGFR (23). Knockdown of RAB7 served as a control to determine whether it is the spatial localization of the receptor or the duration of the viable EGF·EGFR complex. Using these tools, we can assess the affect of accumulating the EGFR at distinct subcellular locations.

The sequences of the siRNA oligos used to attenuate RAB7 and TSG101 expression in these studies have been described previously (23, 25). Their specificity has been validated by rescuing the phenotypes with mutant forms of the protein that are resistant to knockdown.

Transfection of HeLa cells with these siRNA attenuated expression of RAB7 and TSG101 to less than 10% of normal levels (Fig. 4*A*). Further, knockdown of either RAB7 or TSG101 delayed EGF·EGFR degradation as measured by the

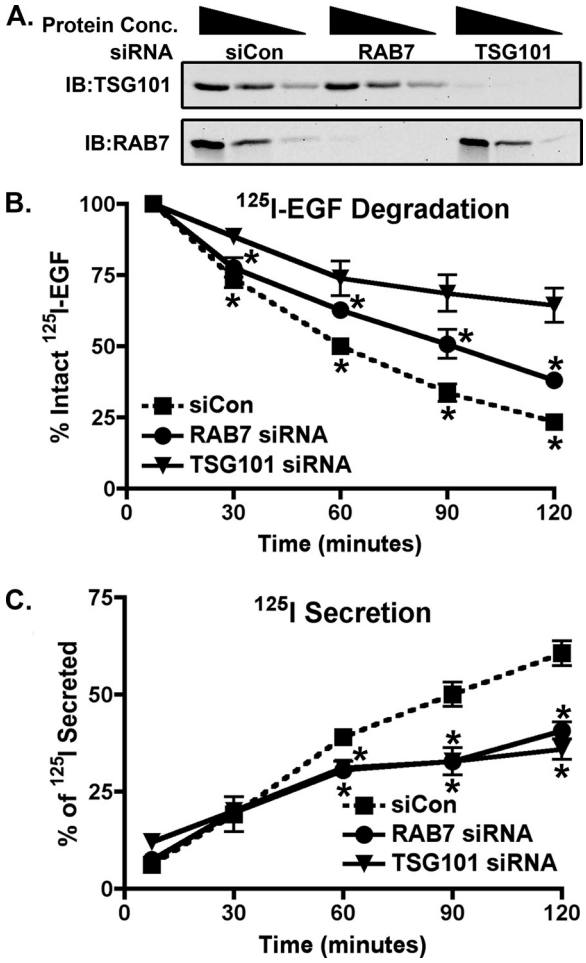

FIGURE 4. **Knockdown of either RAB7 or TSG101 results in attenuated kinetics of degradation of ^{125}I-EGF.** HeLa cells were transfected with either control siRNA (siCon) or siRNA targeting either RAB7 or TSG101. *A*, representative immunoblot (*IB*) analysis indicating the extent of RAB7 and TSG101 knockdown 72 h post-transfection. Serial dilutions of each cell lysate (25 mg, 12.5 mg, and 6.25 mg) were resolved by 12% SDS-PAGE, transferred to nitrocellulose, and immunoblotted with antibodies against either TSG101 (Genetex) or RAB7 (Sigma). *B* and *C*, 72 h post-transfection, cells were incubated at 37 °C with ^{125}I-EGF for 7 min and, following washing to remove unbound radioligand, were incubated in radioligand-free media for the indicated times. At each time point the medium was collected to determine the levels of secreted ^{125}I. In addition, cell lysates were harvested, and intact radioligand was precipitated with trichloroacetic acid. Data are plotted as the percentage of intact ^{125}I-EGF for each time point (*B*) or the percentage of ^{125}I-EGF that was secreted into the media at each time point (*C*) (mean ± S.E., $n = 4$). *, $p < 0.05$ **; $p < 0.10$; calculated by a paired Student's *t* test.

rate of ^{125}I-EGF degradation (Fig. 4*B*) and ^{125}I secretion into the media following degradation of the radioligand (*C*). Knockdown of TSG101 inhibited the rate of ^{125}I-EGF degradation to a greater extent than knocking down RAB7. However, knockdown of either protein was equally effective in inhibiting the secretion of ^{125}I, a process that occurs following lysosomal degradation of the protein. This may reflect differences in how RAB7 and TSG101 knockdown disrupts trafficking in the endocytic pathway. Knockdown of RAB7 may permit partial degradation of the ^{125}I-EGF because of the more acidic environment of the late endosome. Thus, the partially intact ^{125}I-EGF may not be precipitated in our assay (Fig. 4*B*), but the protein degradation may not be sufficient for secretion of the partially degraded radioligand out of the cell (*C*). The assays used likely explain the apparent difference in efficacy of the two proteins.

It has been demonstrated previously using electron microscopy that knockdown of TSG101 and RAB7 enriches the ligand-receptor complex at distinct subcellular locations (the limiting membrane of the late endosome and the ILVs of the late endosome, respectively (23, 25)). To determine quantitatively if the ^{125}I-EGF·EGFR complex accumulated differentially in siRNA-transfected cells, we examined biochemically the endosomal distribution of the ^{125}I-EGF·EGFR complex in TSG101 and RAB7 siRNA-treated cells (Fig. 5). Cells were loaded with ^{125}I-EGF and chased with radioligand-free media. Cells were collected and early, and late endosomes were resolved using sedimentation velocity centrifugation with Percoll gradients, as described in Fig. 1. Density beads and endosome specific proteins were used to verify the identity of the fractions. Low density fractions (R_f ~0.3, 1.040 g/ml) corresponded to early endosomes and higher-density fractions (R_f ~0.9, △ = 1.080–1.109 g/ml) correspond to late endosomes (10).

Preliminary experiments in untransfected HeLa cells indicated a time-dependent progression of the ^{125}I-EGF·EGFR complex from the early endosome to the late endosome. By 120 min after treatment, less than 75% of the starting amount of radioactivity remained, with minor peaks at densities corresponding to early and late endosomes (data not shown).

On the basis of these findings in untransfected HeLa cells, we chose the 120-min time point to examine the endosomal distribution of the EGF·EGFR complex in siRNA-transfected cells (Fig. 5, *A*–*C*). Distribution of radioactivity in cells transfected with control siRNA (*siCon*) established the base line distribution of ligand-receptor complexes (Fig. 5*A*) and was indistinguishable from untransfected cells (data not shown). Cells with attenuated expression of RAB7 showed a large peak of radioactivity in higher-density fractions corresponding to the late endosome (Fig. 5*B*). This is consistent with our previous report that loss of RAB7 causes the EGF·EGFR complex to accumulate in the intraluminal vesicles of the late endosome (23). Knockdown of TSG101 caused ^{125}I-EGF to accumulate at a range of densities ranging from R_f ~0.3–0.9 (Fig. 5*C*). This likely reflects the incomplete maturation of early endosomes into late endosomes, resulting in endosomes of a wide range of densities (25). With both RAB7 and TSG101 knockdown, there was approximately a 2-fold increase in the total cell associated radioactivity as compared with the siCon-transfected cells (Fig. 5*D*). This is consistent with what was observed in the analysis of ^{125}I-EGF secretion following RAB7, TSG101, and siCon transfection (Fig. 4*C*).

Our biochemical data, along with previous reports, indicate that although knockdown of RAB7 and TSG101 both delay the degradation of the EGF·EGFR complex, they do so at different stages in the endocytic pathway.

Knockdown of TSG101 but not RAB7 Prolongs EGFR Phosphorylation—To assess how these changes in trafficking affected signaling, we examined the kinetics of EGFR phosphorylation and degradation following RAB7 and TSG101 knockdown. Following ligand binding, EGFR monomers dimerize, their kinase domains become active, and the kinase domain of one EGFR monomer transphosphorylates the tyrosine residues

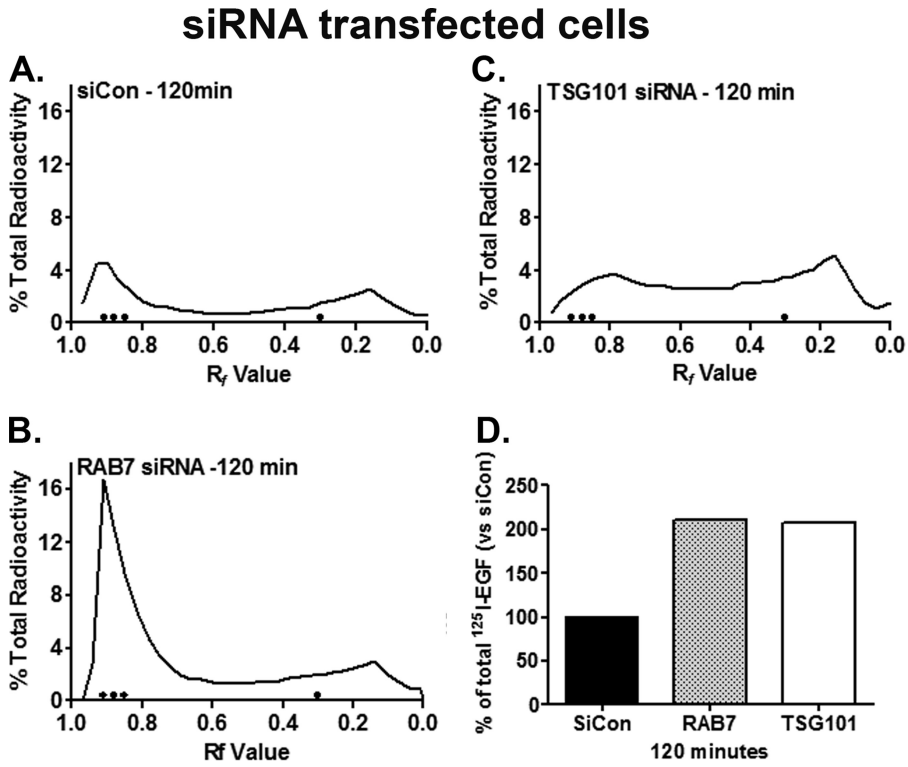

FIGURE 5. **RAB7 knockdown causes ^{125}I-EGF to accumulate in high density endosomes and TSG101 knockdown causes ^{125}I-EGF to accumulate in endosomes of a range of densities.** The endocytic accumulation of the ^{125}I-EGF·EGFR complex was assessed by pulse-labeling cells with ^{125}I-EGF. Following 120 min of chase with radioligand-free media, postnuclear supernatant was prepared from HeLa cells transfected with either control siRNA (siCON) (*A*), siRNA targeting either RAB7 (*B*), or TSG101 (*C*). Data were plotted as the relative distribution of ^{125}I in each fraction and were normalized to the total radioactivity. Shown are representative graphs from four independent experiments. *D*, plot of the relative total radioactivity in transfected HeLa cells following incubation for 120 min at 37 °C. Circles along the *x* axis indicate the distribution of density beads (from lowest to highest Rf: 1.040 g/ml, 1.055 g/ml, 1.069 g/ml, and 1.109 g/ml). Early endosomes migrate at 1.035–1.042 g/ml. The heavier late endosomes sediment with a density of 1.048–1.060 g/ml.

of its receptor pair. Thus, monitoring EGFR phosphorylation serves as an assay for the duration of EGFR activity.

Serum-starved cells were treated with EGF (10 ng/ml) for 0–180 min, and total and phosphorylated EGFR (pY1068) was measured by immunoblot analysis (Fig. 6*A*). Densitometric analysis quantified the difference in total EGFR phosphorylation (Fig. 6*B*) and the phosphorylation relative to the total amount of receptor present (*C*).

We observed unexpected kinetic differences between EGFR dephosphorylation and EGFR degradation. Knockdown of RAB7 produced no change in the kinetics of EGFR phosphorylation and dephosphorylation compared with siCon control cells, but the kinetics of receptor degradation were slowed.

TSG101 knockdown cells had dramatically slowed kinetics of EGFR dephosphorylation without any significant difference in the rate of EGFR degradation. One possible explanation is that only a small percentage of the total receptor is phosphorylated and that the phosphorylated receptor traffics differently than the dephosphorylated receptor.

Importantly, despite changes in the steady-state distribution of the EGFR with either RAB7 or TSG101 knockdown and decreased total EGFR with TSG101 knockdown, levels of maximal receptor phosphorylation were comparable in all three conditions.

Prolonged EGFR Phosphorylation Induces Apoptosis in HeLa Cells—Having established a model system, we examined whether EGFRs retained at the limiting membrane of the endosome could induce apoptosis. Cells transfected with TSG101, RAB7, or control siRNA were grown in either growth medium (with serum), DMEM, or DMEM plus 10 ng/ml EGF (Fig. 7*A*). Over the course of 72 h, EGF profoundly reduced the viability of TSG101 knockdown cells. Cells transfected with TSG101 siRNA and grown in the presence of EGF became rounded in morphology and showed increased cell death. In contrast, TSG101 knockdown cells grown in either growth media or DMEM showed no morphological abnormalities or decreased survival. Further, EGF treatment of the siCon control or RAB7 knockdown cells had no detectable effect on cell morphology or survival.

To quantify these cellular changes, we used the MTT assay to measure cell viability at 24 and 48 h (Fig. 7*B*). EGF-dependent cell growth at 24 h was similar among control (siCon), RAB7 knockdown, and TSG101 knockdown cells. At 48 h, control (siCon) and RAB7 siRNA-transfected cells maintained their modest growth enhancement, as shown by the dose-dependent increase in the number of viable cells. In contrast, and consistent with our microscopic findings, TSG101 knockdown cells showed a dose-dependent decrease in the number of viable cells at 48 h (Fig. 7*B*). We determined that TSG101 knockdown cells underwent apoptosis in response to EGF on the basis of the appearance of cleaved PARP, an apoptosis marker (Fig. 7*C*). RAB7 knockdown cells, which sequesters the EGFR in the intraluminal vesicles of the late endosome, and the siCon control cells, which process the EGFR normally, showed no increase in the cleaved form of PARP in response to EGF.

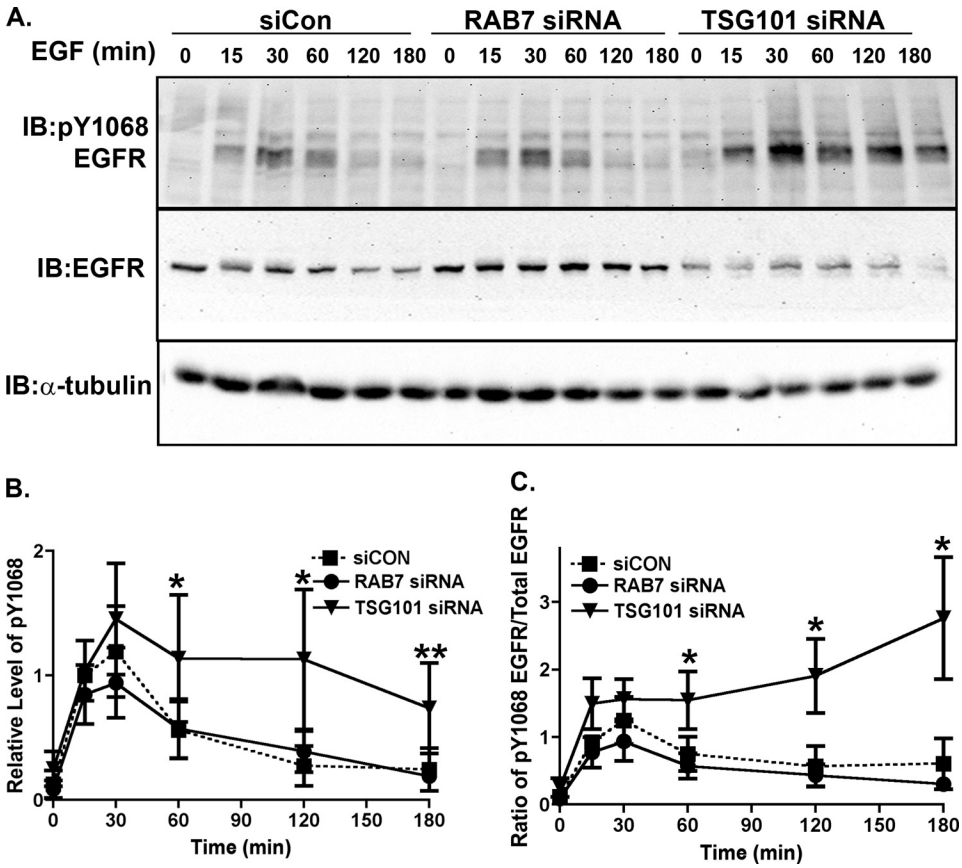

FIGURE 6. **Knockdown of TSG101, but not RAB7, prolongs EGFR signaling.** HeLa cells were transfected with either control siRNA (siCon) or siRNA targeting either RAB7 or TSG101. Following recovery from transfection (72 h), cells were serum-starved for 2 h and then treated with 10 ng/ml EGF for the indicated amounts of time. *A*, cell lysates were prepared, and equivalent amounts of protein were resolved by 7.5% SDS-PAGE, transferred to nitrocellulose, and immunoblotted (*IB*) with antibodies for either phosphorylated EGFR (*pY1068 EGFR*), EGFR, or α-tubulin. Shown is a representative blot of an experiment repeated four times. *B* and *C*, densitometric readings from four independent experiments were quantified using ImageJ software and normalized to the intensity of the 15-min time point in siCon cells for phosphorylated EGFR or to the 0-min time point for total EGFR. Data are presented as the mean ± S.E. *, $p < 0.10$; **, $p < 0.05$; calculated by a paired Student's *t* test.

DISCUSSION

We have demonstrated previously that EGF induces MDA-MB-468 cells to undergo apoptosis regulated by the intracellular localization of the EGF·EGFR complex (8). In this study, we demonstrate in MDA-MB-468 cells that the activated EGF·EGFR complex accumulates on the limiting membrane of the early endosome with the phosphotyrosines of the carboxyl terminus of the receptor exposed to the cytoplasm. From these data, we developed the hypothesis that the accumulation of EGFRs on the limiting membrane of the endosome is sufficient to induce ligand-mediated apoptosis.

To test our hypothesis, we used HeLa cells and disrupted EGFR endocytic trafficking using a pharmacological agent (monensin) to prevent trafficking of the EGFR beyond the endosome, resulting in the accumulation of the active receptor at the endosome. Following treatment with monensin, we observed an EGF-dependent decrease in viable cells, indicating that retention of the activated EGFR in the endosome was sufficient to compromise cell viability. We used an RNAi strategy to demonstrate that the endosomal orientation of the receptor was critical to EGF-induced apoptosis. Knockdown of TSG101, which keeps the receptor on the limiting membrane of the endosome with the carboxyl terminus oriented toward the cytoplasm, led to a similar trend of apoptosis. However, RAB7 knockdown, which allows the ligand-receptor complex to be sequestered in the ILVs with the carboxyl terminus no longer accessible to downstream effectors, did not yield EGF-dependent induction of apoptosis.

Importantly, with both the pharmacological and RNAi strategies, the cells underwent apoptosis in response to EGF, but not in serum-free or growth media, confirming that apoptosis required EGFR signaling. These data indicate that the spatial localization of the active EGFR on the limiting membrane of the endosome is sufficient to signal apoptosis.

Consistent with the increase in apoptosis, we also observed that TSG101 knockdown resulted in prolonged ligand-dependent EGFR phosphorylation, whereas RAB7 knockdown did not. Because knockdown of either protein causes slowed kinetics of degradation but at different subcellular locales, this is likely due to receptor dephosphorylation occurring in the ILV of the late endosome/multivesicular body. This may be the result of an ILV-specific resident phosphatase, ligand dissociation and subsequent receptor kinase inactivation, or the sensitivity of tyrosine phosphorylation to the acidic ILV.

Apoptosis is often underappreciated as one of the physiologically relevant EGFR-mediated changes in cell biology. It may be an important protective feedback mechanism when EGFR signaling goes awry. That is, the EGFR does not nor-

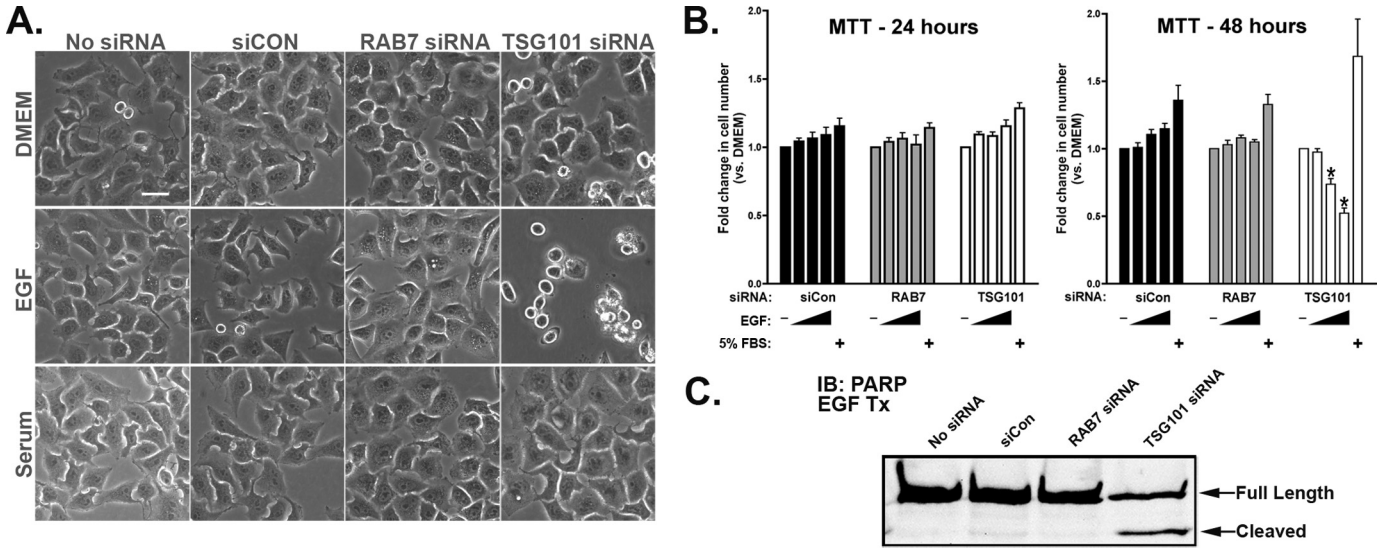

FIGURE 7. **Retention of the EGF·EGFR complex on the limiting membrane of the endosome induces apoptosis.** *A*, siRNA-treated cells were grown in either growth media, DMEM alone, or DMEM with 10 ng/ml EGF for 48 h. Shown are representative phase contrast images of cell morphology collected using a ×40 objective on a Nikon Eclipse TE-2000U microscope. *Scale bar* = 10 μm. Shown are representative images from an experiment performed three times. *B*, 24 h post-transfection, cells were replated in a 96-well dish and treated with varying concentrations of EGF (0 ng/ml, 0.1 ng/ml, 1.0 ng/ml, 10 ng/ml) or media containing 5% FBS for 24 or 48 h. The number of viable cells were assessed using an MTT assay as described under "Experimental Procedures." Data are plotted as fold change in cell number relative to cells maintained in DMEM without ligand. *, p value < 0.05 as measured by a Student's t test ($n = 4$). *C*, cell lysates from the cells in *B* were prepared, resolved by 7.5% SDS-PAGE, and immunoblotted for PARP. Full-length and cleaved PARP are indicated by the *upper* and *lower arrows*. Shown is a representative image from an experiment performed three times.

mally induce apoptosis as part of the role of the receptor in tissue development but may trigger apoptosis when the cell senses excessive EGFR signaling as a result of EGFR overexpression or defective signal attenuation. Thus, EGFR-mediated apoptosis may be important for maintaining the overall tissue homeostasis.

It has been speculated previously that the EGFR-mediated induction of apoptosis may limit the invasiveness of breast cancer (26). Perhaps our findings could be used to specifically target EGFR-positive cancers by simultaneously stimulating the receptors while inhibiting their endocytic trafficking. If our model were correct, one would predict that cancer cells with higher levels of EGFR expression/activity would be most sensitive to the blockade of EGFR trafficking. Thus, the EGFR-expressing cancer cells would be affected preferentially over normal cells, minimizing side effects.

In addition, this work provides important insight into the basic cell biology of how the endocytic pathway negatively regulates EGFR signaling. There have been at least three models proposed for how signaling by the EGFR is terminated: dephosphorylation of the EGFR, sequestration of the ligand-receptor complex into intraluminal vesicles, or degradation of the receptor. Our strategy of disrupting endocytic trafficking at discrete stages in the pathway allows us to discriminate among these models.

Knockdown of either TSG101 or RAB7 delays EGFR degradation, but only knockdown of TSG101 prolongs signaling, suggesting that receptor degradation by itself is not the key regulatory mechanism. Rather, it appears that sequestration of the ligand-receptor complex is needed to terminate signaling. Keeping the EGFR on the limiting membrane of the endosome prolongs signaling as measured by receptor phosphorylation.

This finding is consistent with the work by Bache *et al.* (27). In their study, the authors knocked down two different ESCRT proteins to selectively accumulate EGFRs at the limiting membrane and in the ILVs of the late endosome. They demonstrated that receptors on the limiting membrane had increased MAPK activity but did not report a change in cell physiology. Because subtle changes in effector activity often do not alter cell physiology, our study provides a context for changes in signal regulation. The induction of apoptosis in a dose-dependent manner indicates that it is mediated through the EGFR. Identification of the specific effector(s) downstream of the activated EGFR in the limiting membrane of the endosome is an important area for further investigation.

For the EGFR, the limiting membrane of the late endosome/multivesicular body may be a logical pharmacological target to trap receptors and enhance their signaling (*i.e.* to promote EGFR-mediated wound healing). Conversely, promoting rapid sequestration of activated receptors into the ILVs may be a useful approach to accelerate termination of receptor signaling (*i.e.* in cancers that overexpress EGFRs). It should be noted that this strategy may need to be modified for other signaling pathways. It was recently reported that sequestration of canonical Wnt signaling potentiates signal transduction by trafficking of glycogen synthase kinase 3 into the ILVs of the late endosome/multivesicular body (28).

Here we provide evidence of a novel cellular feedback mechanism that prevents prolonged EGFR signaling by inducing apoptosis. These findings bring new insights into how endocytic trafficking regulates EGFR signaling.

REFERENCES

1. Olayioye, M. A., Neve, R. M., Lane, H. A., and Hynes, N. E. (2000) *EMBO J.* **19,** 3159–3167

2. Yarden, Y., and Sliwkowski, M. X. (2001) *Nat. Rev. Mol. Cell Biol.* **2,** 127–137
3. Rowinsky, E. K. (2004) *Annu. Rev. Med.* **55,** 433–457
4. Tullo, A. B., Esmaeli, B., Murray, P. I., Bristow, E., Forsythe, B. J., and Faulkner, K. (2005) *Eye* **19,** 729–738
5. Zhang, G., Basti, S., and Jampol, L. M. (2007) *Cornea* **26,** 858–860
6. Sorkin, A., and Goh, L. K. (2009) *Exp. Cell Res.* **315,** 683–696
7. Vieira, A. V., Lamaze, C., and Schmid, S. L. (1996) *Science* **274,** 2086–2089
8. Hyatt, D. C., and Ceresa, B. P. (2008) *Exp. Cell Res.* **314,** 3415–3425
9. Damke, H., Gossen, M., Freundlieb, S., Bujard, H., and Schmid, S. L. (1995) *Methods Enzymol.* **257,** 209–220
10. Kornilova, E., Sorkina, T., Beguinot, L., and Sorkin, A. (1996) *J. Biol. Chem.* **271,** 30340–30346
11. Diaz, R., and Stahl, P. D. (1989) *Methods Cell Biol.* **31,** 25–43
12. Dinneen, J. L., and Ceresa, B. P. (2004) *Traffic* **5,** 606–615
13. Sorkin, A. D., Teslenko, L. V., and Nikolsky, N. N. (1988) *Exp. Cell Res.* **175,** 192–205
14. Hansen, M. B., Nielsen, S. E., and Berg, K. (1989) *J. Immunol. Methods* **119,** 203–210
15. Cailleau, R., Olivé, M., and Cruciger, Q. V. (1978) *In Vitro* **14,** 911–915
16. Filmus, J., Pollak, M. N., Cailleau, R., and Buick, R. N. (1985) *Biochem. Biophys. Res. Commun.* **128,** 898–905
17. Armstrong, D. K., Kaufmann, S. H., Ottaviano, Y. L., Furuya, Y., Buckley, J. A., Isaacs, J. T., and Davidson, N. E. (1994) *Cancer Res.* **54,** 5280–5283
18. Gill, G. N., and Lazar, C. S. (1981) *Nature* **293,** 305–307
19. Kottke, T. J., Blajeski, A. L., Martins, L. M., Mesner, P. W., Jr., Davidson, N. E., Earnshaw, W. C., Armstrong, D. K., and Kaufmann, S. H. (1999) *J. Biol. Chem.* **274,** 15927–15936
20. Ley, K. D., and Ellem, K. A. (1992) *Carcinogenesis* **13,** 183–187
21. Ceresa, B. P., and Bahr, S. J. (2006) *J. Biol. Chem.* **281,** 1099–1106
22. Dinneen, J. L., and Ceresa, B. P. (2004) *Exp. Cell Res.* **294,** 509–522
23. Vanlandingham, P. A., and Ceresa, B. P. (2009) *J. Biol. Chem.* **284,** 12110–12124
24. King, A. C. (1984) *Biochem. Biophys. Res. Commun.* **124,** 585–591
25. Razi, M., and Futter, C. E. (2006) *Mol. Biol. Cell* **17,** 3469–3483
26. Tikhomirov, O., and Carpenter, G. (2004) *J. Biol. Chem.* **279,** 12988–12996
27. Bache, K. G., Stuffers, S., Malerød, L., Slagsvold, T., Raiborg, C., Lechardeur, D., Wälchli, S., Lukacs, G. L., Brech, A., and Stenmark, H. (2006) *Mol. Biol. Cell* **17,** 2513–2523
28. Taelman, V. F., Dobrowolski, R., Plouhinec, J. L., Fuentealba, L. C., Vorwald, P. P., Gumper, I., Sabatini, D. D., and De Robertis, E. M. (2010) *Cell* **143,** 1136–1148